Lab on a Chip



Cite this: *Lab Chip*, 2011, **11**, 1995

www.rsc.org/loc

**PAPER**

# A new floating electrode structure for generating homogeneous electrical fields in microfluidic channels†

**Loes I. Segerink,* Ad J. Sprenkels, Johan G. Bomer, Istvan Vermes and Albert van den Berg**

***Received 8th October 2010, Accepted 6th January 2011***
**DOI: 10.1039/c0lc00489h**



In this article a new parallel electrode structure in a microfluidic channel is described that makes use of a floating electrode to get a homogeneous electrical field. Compared to existing parallel electrode structures, the new structure has an easier production process and there is no need for an electrical connection to both sides of the microfluidic chip. With the new chip design, polystyrene beads suspended in background electrolyte have been detected using electrical impedance measurements. The results of electrical impedance changes caused by beads passing the electrodes are compared with results in a similar planar electrode configuration. It is shown that in the new configuration the coefficient of variation of the impedance changes is lower compared to the planar configuration (0.39 *versus* 0.56) and less dependent on the position of the beads passage in the channel as a result of the homogeneous electrical field. To our knowledge this is the first time that a floating electrode is used for the realization of a parallel electrode structure. The proposed production method for parallel electrodes in microfluidic channels can easily be applied to other applications.

## Introduction

Electrical impedance measurements of single cells in microfluidic chips are used for a variety of applications, such as diagnostic purposes,[1–3] drug screening,[4,5] cell characterization[6–8] and environmental issues.[9] The measurement of the electrical impedance is a label free method that measures the dielectric properties of the cells or particles in the measurement volume.

Counting of single particles in suspension was firstly done with the use of a Coulter counter,[10] measuring the DC resistance through an orifice. Based on this system, techniques have been developed that use AC signals to measure the electrical properties of cells.[11] Recently, systems for electrical impedance measurements have been miniaturized by integrating the electrodes in the walls of the microchannel,[8] resulting in so-called microfluidic impedance cytometers.[12,13] These microfluidic impedance cytometers have the same advantages as other lab on a chip systems, like a small sample volume, reduction of costs and the possibility to integrate multiple processes. Furthermore it is possible to incorporate optical analysis in the system as well.[3,9]

Several electrode configurations are possible in a microfluidic impedance cytometer with a different number of electrodes. Some microfluidic impedance cytometers use a differential measurement between two electrode pairs into two successive channel parts,[3,9,14–17] while other designs consist of only one electrode pair.[2,18] A differential measurement has the advantage that the electrical impedance change caused by a passing cell is measured with respect to the surrounding electrolyte, such that the influence of environmental changes are reduced and that the speed of the cell can be determined.[16] However, to get reliable results, the cell concentration cannot be too high, since the probability of detecting multiple cells simultaneously increases.

Another important difference that can be made in the electrode configuration is the position of the electrodes with respect to each other. For instance the microfluidic cytometer can have a planar or a parallel electrode configuration. In a planar electrode configuration, two electrodes are positioned at the same side of the channel with an interelectrode distance of several tens of μm. The electrical field distribution between the planar electrodes is inhomogeneous. Due to this inhomogeneity, the position of the particle between the electrodes influences the amount of the electrical impedance change.[13,16,17] This can also explain the relatively large variation we found in the electrical impedance change for the cells passing planar electrodes.[2] Furthermore the relative electrode impedance change caused by a cell is less, compared to the changes measured with systems consisting of parallel electrodes.[16,19] Using a planar configuration in combination with hydrodynamic focusing reduces the position dependency and increases the sensitivity.[17] However, the complexity of the microfluidic chip consisting such focusing system is substantially increased compared to our approach.

Systems with parallel (top-bottom) electrodes in microchannel have already been reported.[3,14,15,18] In these systems an additional layer of for instance polydimethylsiloxane[18] or polyimide[14] is

*BIOS—Lab on a Chip group, MESA+ Institute for Nanotechnology, University of Twente, P.O. box 217, 7500 AE Enschede, The Netherlands. E-mail: l.i.segerink@utwente.nl*

† Published as part of a LOC themed issue dedicated to Dutch Research: Guest Editor Professor Sabeth Verpoorte.

incorporated between two glass substrates both containing the electrodes. The alignment of the electrodes is critical and connection with the electrodes has to be made at both sides of the microchannel, making the fabrication more elaborate than that of planar electrodes. Furthermore the sidewalls of the channel are formed by an additional layer, consisting of a different material. In another embodiment instead of a top-bottom electrode configuration liquid electrodes[1] at the sidewalls of the channel are used. However, according to simulations the relative electrical impedance change is less compared to top-bottom electrode configurations.[1,16,19]

In this paper we describe a new process for the fabrication of top-bottom electrodes that combines the ease of fabrication of planar electrodes with the higher sensitivity of the parallel configuration. In only one extra processing step compared to the fabrication of planar electrodes, a floating electrode opposite of two planar electrodes in the channel is realized. The proposed system has a sensitivity comparable to other published top-bottom electrode systems, but a much easier fabrication process. With this new parallel electrode configuration, the electrical impedance changes of single polystyrene beads are measured and the results are compared with an existing planar configuration. First we describe the theory and concept of the new chip design. Next the newly developed production process is described, followed by electrical characterization of the microfluidic chip and detection of beads passing the electrode using electrical impedance measurements. Subsequently, the results of these measurements are discussed in detail and compared with results obtained with a planar electrode configuration. Finally some conclusions are given.

## Theory

The concept of the floating electrode structure is shown in Fig. 1. It consists of three electrodes: two connecting electrodes on the upper side of the microfluidic channel and one floating electrode on the bottom of the channel. The floating electrode merely functions as a lead between both connecting electrodes. Since AC signals are used to measure the electrical impedance, no charge built up can occur on the floating electrode. Advantages of this floating electrode structure are that electrical connections are only necessary on one side of the chip and the sidewalls of the microfluidic channels consist of the same material as the substrates. Furthermore the production process does not involve difficult alignment steps as compared to reported processes for parallel electrodes. It uses the ease of fabrication of the planar electrodes with the addition of just one processing step.

The total electrical impedance that is measured between the two top electrodes is the sum of the electrical impedance between electrode pair 1 and electrode pair 2. When a suspension of particles is added, it is not clear whether a change in electrical impedance is caused by a particle passing electrode pair 1 or electrode pair 2. Furthermore a larger change in the electrical impedance can be caused by two or more small particles that simultaneously pass both electrodes pairs or by one larger particle that passes one electrode pair. Therefore it is necessary to detect only particles between electrode pair 1 and measure only the fluid between electrode pair 2. This can be achieved by the addition of a second channel as shown in Fig. 1(c). However, to prevent particles to enter electrode pair 2, the fluidic connection between both electrode pairs should be blocked. This blocking can easily be accomplished by introduction of a drop of UV curing glue in the UV-glue hole, as shown in Fig. 1(c).

The microfluidic chip can be modelled by a simplified equivalent circuit model (see Fig. 1(b)). At every electrode–electrolyte interface there is a double layer capacitance ($C_{DL}$). In our microfluidic chip, there are in total four double layer capacitances that are dominant at low frequencies in the bode plot.[13,20] The electrolyte resistance ($R_{el1}$ and $R_{el2}$), in our case the resistance of the fluid between both electrode pairs, plays a role at intermediate frequencies, resulting in a plateau in the bode plot.[20] The detection of particles can best be done with a measurement frequency at this resistive plateau well below 1 MHz,[16,21] since at these frequencies particles and cells behave like insulating spheres. In this case, a particle or cell causes a change in the electrical impedance, when passing along an electrode pair. For low volume fractions ($\Phi \ll 1$), this change can be described by a simplified form of the Maxwell Mixture equation:[13,22]

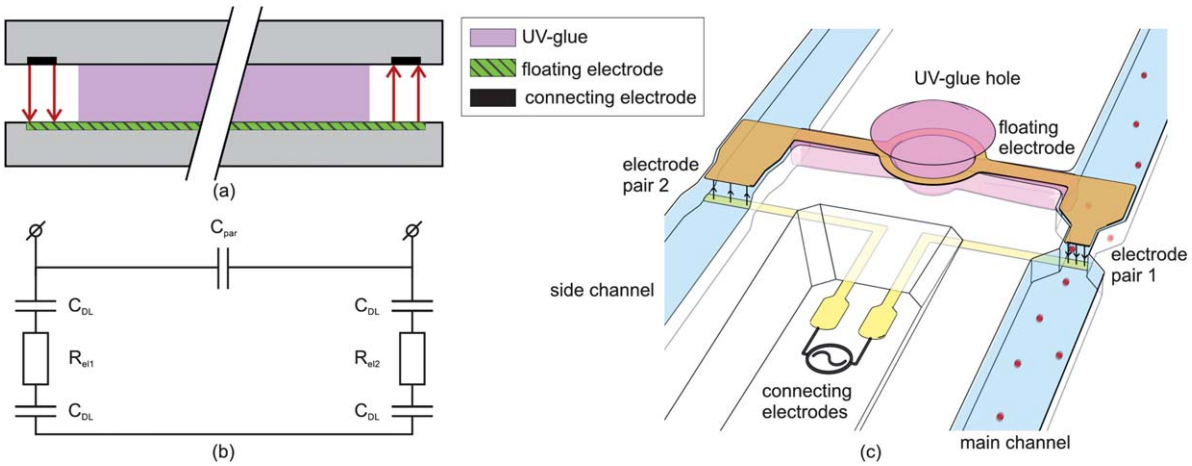


**Fig. 1** (a) Schematic illustration of the floating electrode with (b) the simplified equivalent circuit model. $C_{DL}$ is the double layer capacitance, $C_{par}$ is the parasitic capacitance and $R_{el1}$ and $R_{el2}$ are the electrolyte resistances between electrode pair 1 and 2 respectively. (c) Simplified illustration of chip design type 2. The electrode area of electrode pair 2 of type 2 is 7 times the size of electrode pair 2 of type 1 (not shown).

 

$$\rho_{eq} = \rho_{bge}\left(1 + \frac{3\Phi}{2}\right) \quad (1)$$

with $\rho_{eq}$ the equivalent resistivity of the electrolyte with a particle in it and $\rho_{bge}$ the resistivity of the background electrolyte. At frequencies well above those of the resistive plateau, the bode plot is mainly influenced by the parasitic capacitances ($C_{par}$) of the system.[23]

## Method

### Chip design and fabrication

The schematic diagram of the fabrication is shown in Fig. 2. Compared to the fabrication of planar electrodes that was previously reported,[2] this process contains only one additional step. The microfluidic chips were made of two 500 μm thick 100 mm Borofloat glass wafers. In the top wafer the microfluidic channels with floating electrodes were made. This wafer was covered with sputtered Cr and Au layers; the Cr layer acts as an adhesion layer for Au. This step was followed by a photolithography step and wet etching of the Au and Cr layers. Subsequently the microfluidic channel was isotropically etched in a 25% HF solution. In the next step the floating electrode was realized by placing a shadow mask on top of the photoresist, followed by sputtering of Ta and Pt forming the floating electrode. Next access holes were powderblasted from the back using a photopatternable foil. On the bottom wafer Pt electrodes were realized that form the connecting electrodes to the measurement setup. These were prepared by etching a recess with buffered HF, after a photolithography step. The recess was filled with sputtered Pt with Ta as an adhesion layer (140 nm). In the next step the photoresist was removed, leaving a glass surface with embedded electrodes, which was bonded to the channel side of the top glass wafer using fusion bonding. Finally both bonded wafers were diced into separate chips.

Two types of microfluidic chips have been designed, each having a microchannel with a depth of 18 μm. Due to the floating electrode configuration, the chip consists of two parallel electrode pairs. It is not desirable to have both electrode pairs in the same fluidic channel, since there is a probability that more than one particle is simultaneously detected between both electrode pairs disturbing the impedance measurement. Therefore the second electrode pair is separated from the first electrode pair by use of an additional microfluidic channel. The microchannel containing electrode pair 1 is filled with the suspension containing the particles, while the other channel only contains a background electrolyte. In this way the particles are only detected between electrode pair 1. In both chip designs, the microchannel tapers to a width of 42 μm at the electrode area of electrode pair 1, while at both electrode pairs the width of the active electrodes that span the microchannel is 20 μm. The difference between both chip designs is the electrode area of the second electrode pair. The electrode area of electrode pair 2 is equal to that of electrode pair 1 in the first design and about 7 times larger in the second chip design. Since the particles are measured between electrode pair 1, it is expected that the increase of the electrode area of electrode pair 2 improves the sensitivity as a result of the decreased impedance. In Fig. 1(c) design 2 is shown.

Besides the additional step in the fabrication, one channel in the chip needs to be blocked before experiments can be done. The floating electrode is sputtered on the bottom of the channel, implicating that initially there needs to be a microfluidic channel between both electrode pairs. As already mentioned, such liquid connection is not desirable in the final setup, since particles may enter the region between both electrode pairs. Therefore this connecting channel is designed with an additional access hole, such that it can be filled with UV curing glue. For the gluing Loctite 358 was used and when exposed 20 s to UV radiation of 365 nm it cures. A small drop of glue was put into the access hole and after several seconds the UV source (ELC-403, Electro-Lite Corporation) was turned on, causing the glue to cure instantly.

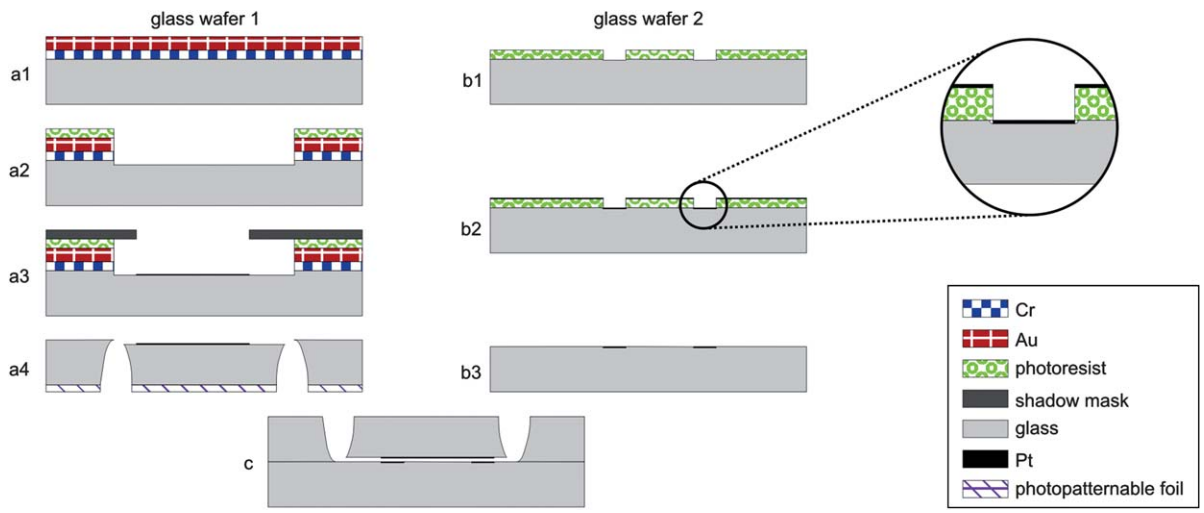


**Fig. 2** Schematic diagram of the fabrication. Glass wafer 1 is firstly sputtered with Cr and Au layers (a1). By means of photolithography and etching, the microfluidic channel is formed (a2). Next a shadow mask is used for the sputtering of the floating electrode on the bottom of the channel (a3). After removing several layers, access holes are powder blasted from the back (a4). On glass wafer 2, the embedded connecting electrodes are formed using a lift-off technique (b1, b2 and b3). Finally both glass wafers are bonded together (c).

### Measurement set-up

For all experiments the chip was put into a chip holder, such that reliable fluidic and electrical connections could be made. The chip holder contains screw threads which are aligned with the access holes of the microfluidic chip. Using a Harvard PHD2000 syringe pump, fluid was pumped through the chip *via* a glass capillary (inner diameter 148 μm) and connected to the microfluidic chip using Upchurch nuts and ferrules (Upchurch Scientific).

Two types of experiments were performed. The first study involves the measurement of the frequency characteristics of both microfluidic chip types. For this purpose the chips were filled with background electrolyte and a bode plot from 100 Hz to 40 MHz was made using a HP impedance/gainphase analyzer type HP4194A, controlled by LabVIEW (7 Express, version 7.0, 2003, National Instruments).

In the second study beads suspended in background electrolyte were detected using electrical impedance measurements. From the results of the first study, the optimal measurement frequency was determined. The actual impedance measurements were done using a HF2IS impedance spectroscope in combination with the HF2CA current amplifier (both Zurich Instruments, Zurich, Switzerland). In Fig. 3 a schematic diagram of the electrical impedance measurement setup is shown. The HF2IS impedance spectroscope was used to generate the excitation signal (1 $V_{PP}$, 500 kHz) as well as to measure the voltages at two inputs. An oscilloscope (Agilent Technologies, type DSO3062A) was connected to the impedance spectroscope for verifying the excitation signal. The first input measured the excitation voltage across both electrodes in the microchannel, while the other input measured the output signal from the HF2CA current-to-voltage converter and thus indirectly the current through the microfluidic chip. In this way, a four point impedance measurement was performed. Both input signals were captured with a sample rate of 899 Hz and used for analysis on a laptop using Matlab (R2007B, version 7.5.0.342, 2007, the MathWorks Inc). In Matlab the electrical impedance was calculated from both signals. In addition, the program was used for the calculation of the peak heights in the same way as described in the previous work.[2] During all measurements, the chip was mounted on an inverted microscope (Leica CTR 6000, Leica Microsystems, Wetzlar, GmbH, Germany).

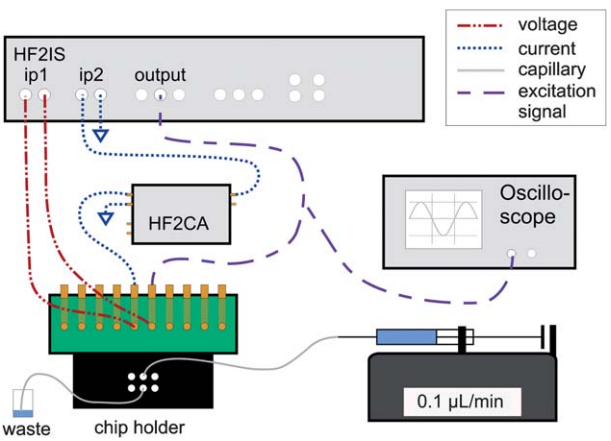


**Fig. 3** Schematic diagram of the measurement set-up. The chip holder makes fluidic and electrical connection to the chip. In this diagram, the inlet and outlet are located underneath the middle two screw threads and the electrodes of the chip are connected to the middle four electrodes on the chip holder. So each electrode on the microfluidic chip has two electrical connections on the chip holder making a four point measurement possible. Input 1 (ip1) of the HF2IS measures the voltage across the chip, while input 2 (ip2) measures *via* the HF2CA the current through the chip.

### Samples

Polybead Polystyrene Violet dyed beads with a diameter of 3 μm and Polybead Polystyrene Black dyed beads with a diameter of 6 μm, both obtained from Polysciences Inc (Warrington, Pennsylvania USA) were used during the experiments. The beads were suspended in Ferticult™ Flushing medium (chemically balanced salt solution, HEPES buffered with 0.4% HSA, purchased from Fertipro NV (Beernem, Belgium)) with a specific electrical conductivity of 1.4 S $m^{-1}$.

## Results and discussion

The microfluidic channels in the chip were isotropically etched in the glass substrate, resulting in a channel width approximately twice the depth of the channel plus the actual width of the mask. For this wet etching process a photoresist layer was used as mask. After the isotropic etching of the microfluidic channel, the photoresist layer was not removed, but also used as mask for the sputtering of the floating electrode. As a result of this procedure, the width of the floating electrode is restricted by the size of the photoresist layer. In our designs, the size of the mask at the electrode pair has a width of 6 μm. From measurements on realized chips, the actual width of the floating electrodes amounted to about 15 ± 2 μm. So in the case of isotropically etching, the floating electrode does not entirely span the bottom of the microchannel but is significantly wider than the width of the mask as a result of the inherent widening of sputtering through a shadow mask.

In both chip designs, electrode pairs 1 and 2 are located in a different microfluidic channel. One electrode pair is used for detection of particles in the fluid, while the other measures only the electrical impedance of the fluid and acts actually as

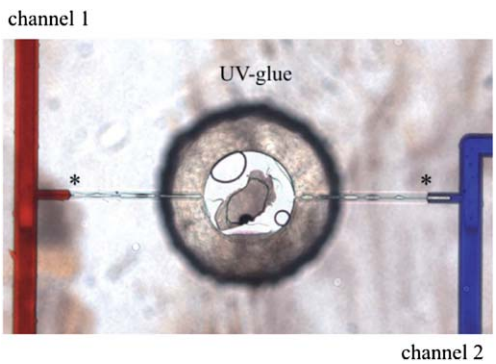


**Fig. 4** Blocking of the interconnecting channel that is used as host for the floating electrode, using UV curing glue. The asterisks indicate the crossings between the fluid and the cured UV glue.

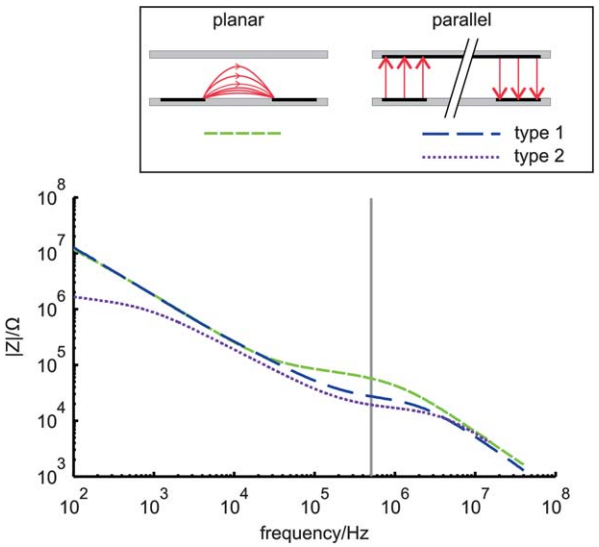


**Fig. 5** The measured frequency response of the real electrical impedance signal for three chip designs each with a different electrode configuration. The vertical line indicates the optimal measurement frequency. Parallel electrode configuration type 2 has a 7 times larger electrode area of electrode pair 2, compared to parallel electrode configuration type 1.

a connection to the outer world. An interconnecting channel is needed to host the floating electrode and this channel has to be blocked for liquids before experiments can be done which is achieved with UV glue. Fig. 4 shows the blocking mechanism in chip design 1 as an example. Both channels containing the red and blue liquid are clearly separated from each other.

### Characterization of the chips

In Fig. 5 the results of the impedance measurements of three different chip designs are shown. Parallel designs 1 and 2 and the chip with a planar electrode configuration used in the previous work[2] were filled with background electrolyte and the averages of 50 measurements are shown. The influence of the electrical double layer and the parasitic capacitances can be clearly seen for every electrode design at low and high frequencies respectively. The value of the resistive plateau differs for every chip. The planar electrode configuration has a higher resistive plateau than the two parallel electrode configurations. As expected, chip type 2 has a lower resistive plateau compared to chip type 1, since the area of electrode pair 2 is larger in design 2, decreasing the overall impedance. The chosen measurement frequency of 500 kHz used for the detection of particles is appropriate for the three designs, which all have the resistive plateau at this frequency.

### Detection of beads

First electrical impedance measurements with parallel electrode configuration type 1 were performed. By measuring the electrical impedance and simultaneously observing the video images taken by the microscope camera, every 6 μm bead that passed the electrode was visually and electrically detected. Fig. 6 shows a typical example of the measured signal. The electrical impedance changes of 146 beads have been measured and amounted to 9.3 ± 3.6 Ω.

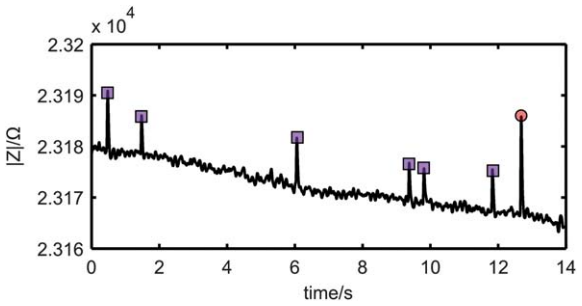


**Fig. 6** An example of the raw electrical impedance signal with the new parallel electrode configuration. The peaks with the squares indicate the passage of one 6 μm bead, while the peak with the circle is caused by the passage of two 6 μm beads simultaneously which event was observed by visual inspection.

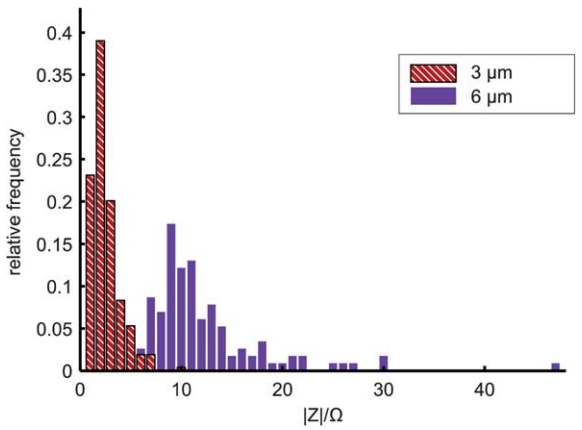


**Fig. 7** A histogram of the impedance changes caused by 3 and 6 μm beads.

Subsequently, 6 μm beads have been detected with parallel electrode configuration type 2, resulting in an impedance change of 12.8 ± 5.9 Ω ($n$ = 115). This experiment was also performed with 3 μm beads (3.0 ± 1.4 Ω, $n$ = 264). Fig. 7 shows the impedance changes measured for both 3 and 6 μm beads. The 6 μm beads generate a significant ($p$ < 0.01) larger impedance change than the 3 μm beads, as expected by their size. These results clearly indicate that with the parallel electrode configuration it is possible to distinguish 3 and 6 μm beads from each other.

### Influence electrode configuration

Measurements with electrode configuration type 1 already showed that it is possible to detect 6 μm polystyrene beads in suspension. The same measurements were done with a planar electrode configuration (23.1 ± 12.9 Ω, $n$ = 140) and the parallel electrode configuration type 2 (12.8 ± 5.9 Ω, $n$ = 115). The average value of the electrical impedance change for the planar electrode pair is significantly ($p$ < 0.01) larger than those of the two parallel electrode configurations. This can be explained by the volume fraction of the particle. In the parallel configuration, the measurement volume is about twice that of the planar configuration due to the two electrode pairs in series. Therefore

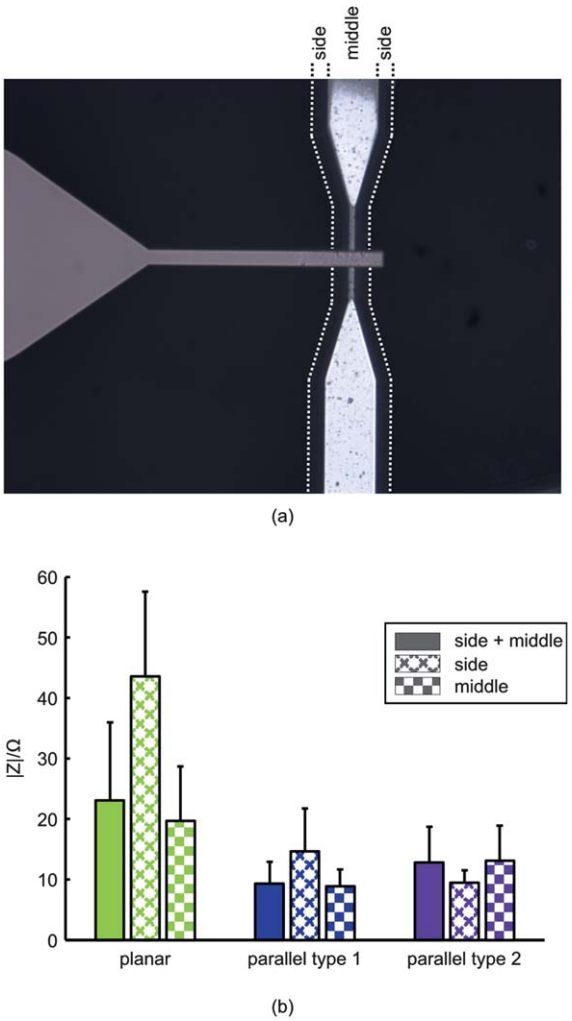


**Fig. 8** (a) A microscope image (differential interference contrast) of the electrode pair 1 of the parallel electrode configuration indicating the side and middle positions of the channel. (b) The influence of the position of the 6 μm bead in the channel. The error bars indicate one standard deviation.

the same particle has a lower volume fraction in the parallel electrode configuration than in the planar one, causing a smaller impedance change (see eqn (1)).

To compare the three electrode configurations, the coefficient of variation was calculated for each electrode configuration, resulting in 0.56, 0.39 and 0.46 for planar, parallel type 1 and parallel type 2 respectively. The large spread for the electrical impedance change in the planar electrode configuration can be explained by the position of the beads in the channel passing the electrodes. Beads that are at the flexion of the microfluidic channel generate significantly larger electrical impedance changes, than beads that flow through the middle of the microfluidic channel (see Fig. 8). At the flexion of the microfluidic channel, the electrical field is the strongest, since the depth of the channel is less. So a particle in this part of the microfluidic channel will cause a higher electrical impedance change.

The difference between type 1 and type 2 of the parallel electrode configuration is a result of the different area of electrode pair 2 that only measures the background electrolyte. As mentioned, we expect better sensitivity when the area is larger, since the impedance at that electrode pair is reduced. The results show that the electrical impedance change is indeed somewhat larger for type 2. However, the coefficient of variation was larger for this electrode configuration.

## Conclusions

A new method for the fabrication of parallel electrodes in a microfluidic chip has been developed, which can be used for a microfluidic impedance cytometer. A floating electrode is used in the new method, making electrical connections only to one side of the chip necessary. With this method, a floating electrode is positioned at the opposite side of the channel relative to the connecting electrodes, creating a parallel electrode configuration. Due to this floating electrode, the fabrication is easier than previously reported methods for the realization of parallel electrode configurations. With the new electrode configuration it was possible to detect polystyrene beads suspended in a fluid. Furthermore the coefficient of variation in electrical impedance change was less for the new configuration compared to a planar configuration, since the position of the beads in the channel has less influence on the impedance change. The new floating electrode structure is not solely useful for electrical impedance measurements, but we think other applications like separation based on dielectrophoresis can also be performed with this floating electrode concept. Future work will be focused on improving the sensitivity of the configuration for instance by using a highly conductive background electrolyte in the additional channel at electrode pair 2.

## Acknowledgements

This research is supported by the Dutch Technology Foundation STW, which is the applied science division of NWO, and the Technology Programme of the Ministry of Economic Affairs. The chip fabrication support by Daniel Wijnperlé and the LabVIEW support from Mathieu Odijk are gratefully acknowledged.

## References

1 A. Valero, T. Braschler and P. Renaud, *Lab Chip*, 2010, **10**, 2216–2225.
2 L. I. Segerink, A. J. Sprenkels, P. M. Braak ter, I. Vermes and A. Berg van den, *Lab Chip*, 2010, **10**, 1018–1024.
3 D. Holmes, D. Pettigrew, C. H. Reccius, J. D. Gwyer, C. Berkel van, J. Holloway, D. E. Davies and H. Morgan, *Lab Chip*, 2009, **9**, 2881–2889.
4 S. Z. Hua and T. Pennell, *Lab Chip*, 2009, **9**, 251–256.
5 D. Malleo, J. T. Nevill, L. P. Lee and H. Morgan, *Microfluid. Nanofluid.*, 2010, **9**, 191–198.
6 Y. H. Cho, T. Yamamoto, Y. Sakai, T. Fujii and B. Kim, *J. Microelectromech. Syst.*, 2006, **15**, 287–295.
7 L. S. Jang and M. H. Wang, *Biomed. Microdevices*, 2007, **9**, 737–743.
8 L. Ghenim, H. Kaji, Y. Hoshino, T. Ishibashi, V. Haguet, X. Gidrol and M. Nishizawa, *Lab Chip*, 2010, **10**, 2546–2550.
9 G. Benazzi, D. Holmes, T. Sun, M. C. Mowlem and H. Morgan, *IET Nanobiotechnol.*, 2007, **1**, 94–101.
10 W. H. Coulter, *Proc. Natl. Electron. Conf.*, 1956, **12**, 1034–1040.
11 R. A. Hoffman and W. B. Britt, *J. Histochem. Cytochem.*, 1979, **27**, 234–240.

 

12 H. E. Ayliffe, A. B. Frazie and R. D. Rabbitt, *J. Microelectromech. Syst.*, 1999, **8**, 50–57.
13 T. Sun and H. Morgan, *Microfluid. Nanofluid.*, 2010, **8**, 423–443.
14 K. Cheung, S. Gawad and P. Renaud, *Cytometry, Part A*, 2005, **65**, 124–132.
15 D. Holmes and H. Morgan, *Anal. Chem.*, 2010, **82**, 1455–1461.
16 S. Gawad, L. Schild and P. Renaud, *Lab Chip*, 2001, **1**, 76–82.
17 R. Rodriguez-Trujillo, O. Castillo-Fernandez, M. Garrido, M. Arundell, A. Valencia and G. Gomila, *Biosens. Bioelectron.*, 2008, **24**, 290–296.
18 D. K. Wood, M. V. Requa and A. N. Cleland, *Rev. Sci. Instrum.*, 2007, **78**, 104301.
19 T. Sun, N. G. Green, S. Gawad and H. Morgan, *IET Nanobiotechnol.*, 2007, **1**, 69–79.
20 H. Morgan, T. Sun, D. Holmes, S. Gawad and N. G. Green, *J. Phys. D: Appl. Phys.*, 2007, **40**, 61–70.
21 K. Asami, *J. Non-Cryst. Solids*, 2002, **305**, 268–277.
22 J. Maxwell, *A Treatise on Electricity and Magnetism*, Clarendon Press, Oxford, 1873.
23 G. R. Langereis, PhD thesis, University of Twente, 1999.